Single Step Electrodeposited Kesterite Cu$_2$ZnSnS$_4$ (CZTS) Thin Films at Low Annealing Temperatures

Bernabe Mari[1*], Miguel Mollar[1], Amany El Nahrawy[2], Suzan Saber[1,2,3], Nagwa Khattab[2], Ali Eid[2], Mohamed Abo-Aly[3] and Feriel Bouhjar[1,4,5]

[1]Design and Manufacturing Institute, Polytechnic University of Valencia, Camino de Vera s/n 46022 Valencia, Spain

[2]National Research Center, 33 El Bohouth St. (former El Tahrir St.), Dokki, Giza, Cairo, Egypt

[3]Chemistry Department, Faculty of Science, Ain Shams University, Cairo, Egypt

[4]Photovoltaic Laboratory, Research and Technology Centre of Energy, Borj-Cedria Science and Technology, Tunisia

[5]Universite de Tunis EL Manar, Campus Universitaire Farhat Hached, Rommana, Tunis, Tunisia

*Corresponding author: Bernabe Mari, Design and Manufacturing Institute, Polytechnic University of Valencia, Camino de Vera s/n 46022 Valencia, Spain, Tel: 585-395-5586; E-mail: bmari@fis.upv.es

Citation: Mari B, Mollar M, Nahrawy AE, Saber S, Khattab N, et al. (2018) Single Step Electrodeposited Kesterite Cu$_2$ZnSnS$_4$ (CZTS) Thin Films at Low Annealing Temperatures. Insights Anal Electrochem Vol.4 No.1:8

Abstract

This paper reports on the growth of quaternary Cu$_2$ZnSnS$_4$ (CZTS) thin films by a single step electrochemical deposition followed by annealing at low temperature. The influence of different annealing atmospheres at constant annealing times (t=45 min) and fixed preparation controlling parameters; i.e., starting materials (precursor metal salts) solution concentration, time of deposition and electrodeposition potential. Structural, compositional, morphological and optical properties as well as photoelectrochemical properties were studied. The films sulfurized during 2 hours, showed a prominent kesterite phase with a nearly stoichiometric composition. Samples were characterized by X-ray diffraction (XRD), scanning electron microscopy (SEM), EDS and UV-VIS-NIR spectrometry. X-ray diffraction and confirmed the formation of pure kesterite CZTS films. SEM shows that films are compact with dense morphology and homogeneous distribution. EDS analyzed the elemental constituents of the quaternary Cu$_2$ZnSnS$_4$ with an apparent Cu deficiency and S rich for the sulfurized samples. From optical study, the energy gap was indexed for the sulfurized samples. Eg=1.52 eV. Under illumination sulfurized CZTS films exhibits negative photocurrent and positive photovoltage values confirming the p-type character of the films.

Keywords: Cu$_2$ZnSnS$_4$; Single step electrodeposition; Thin films; Sulfurization

Introduction

At present, photovoltaic solar cell investigations have rapidly increased due to the higher demand of cleaner energy consumption. In this sense, chalcogenides semiconductors exhibit unique optical, electrical and chemical properties [1-5]. Consequently, in the last years, these compounds have attracted the attention of the scientific community. In particular, the thin film technology has been heavily promoted by the interest in CdTe and CIGS-based solar cells [6-8]. However, these materials contain scarce elements in the earth's crust, such as In, Te and Ga and toxic ones as Cd and Se [9,10]. Cu$_2$ZnSnS$_4$ system (CZTS) that crystallizes kesterite structure is one of the most promising absorber materials for solar cells, because of its low band gap around 1.5 eV and its high absorption coefficient (104 cm^{-1}) [11]. In addition, the absence of toxic elements and incorporation of low cost, abundant and environmentally friendly elements as Zn and Sn, instead of In and Ga [12]. Currently, 12.6% of efficiency record has been achieved using hydrazine-based solution. Shockley–Queisser photon balance calculations display 32.2% of theoretical conversion limit for CZTS solar cells [13]. Thus, it is important to highlight that the CZTS efficiency could improve noticeably and becomes closer to CIGS efficiency (20.1%). In the past, several chemical routes for CZTS synthesis have been studied as well as their thin film deposition [14].

There are various preparation methods of CZTS divided into two main parts; (1) physically vacuum deposition techniques like sputtering [15,16], evaporation [17-19] and pulsed laser deposition (PLD) [20]; (2) chemically based non-vacuum deposition techniques such as electrodeposition [21,22], hydrazine-based solution [23] and sol gel-based methods [24]. Electrodeposition technique is with favorable unique advantages that are low-cost, large area plating, convenient

industrial process, so electrodeposition is highly competitive degree than other manufacturing techniques for CZTS synthesis. Three electrode cell processes are characterized by four main deposition techniques depending upon the starting precursor species of ions. (1) stacked elemental layer approach (SEL), (2) metal alloy electrodeposition (MAE), (3) electrophoretic deposition (EPD), and (4) quaternary electrodeposition (QED).

In each case, a post-deposition annealing step in the presence of a molecular conductor source (chalcogenide) to enhance the growth process. Each process possesses their own merits and drawbacks, and all of them have drawn significant attention as comfortable methods for large area CZTS thin film deposition.

Here, we propose a single-step electrochemical deposition method (SED) to deposit quaternary elements of copper, zinc, tin and sulfur onto ITO substrates. The as deposited CZTS films were further thermally treated in different atmospheres argon and sulfur, respectively; at different temperatures in order to enhance the crystallinity of the prepared films. The physical properties, microstructure and morphology of the as deposited and treated ones were studied by X-ray diffraction. The best structure with the smallest crystal size was further

studied by scanning electron microscopy and EDS. Optical properties were measured in order to calculate the band gap energy and the absorption coefficient. Photoelectrochemical properties were studied also for the sulfurized samples.

Experimental

Methods

CZTS thin-film precursor is grown by single-step electrodeposition using -1.05 V versus saturated calomel electrode (SCE) at RT for 45 min. The CZTS thin films were electrodeposited potentiostatically on ITO substrates. Substrate cleaning process is performed in an ultrasonic using some organic solvents (soap, ethanol, acetone, 15 min each step) in order to obtain uniform and good adherent deposition. Electrochemical baths were formed of an aqueous solution containing $CuSO_4$ (20 mM), $ZnSO_4$ (10 mM), $SnSO_4$ (20 mM) and $Na_2S_2O_3$ (0.2 M).

Tartaric acid is used to adjust pH of the solution at 5.0 and tri-sodium citrate ($Na_3C_6H_5O_7$) was as complexing agent. The precursor films formed were annealed in Ar atmosphere and in sulfur atmosphere **(Table 1)**.

Table 1 Preparation parameters for Cu2ZnSnS4 as grown, annealed in Ar atmosphere and sulfurized.

Annealing atmospheres	Temperature (°C)	Annealing Time (Min)	Potential (V)	pH	Deposition Time (S)
Cu_2ZnSnS_4 - sulfurized	400	45	-1.05	5.0	2700
Cu_2ZnSnS_4 - Annealed in Ar	450	45	-1.05	5.0	2700
Cu_2ZnSnS_4 -as-grown	-	-	-1.05	5.0	2700

Materials characterization

The crystal structure of CZTS is investigated by XRD (Rigaku Ultima IV diffractometer in the Bragg-Bentano configuration) using the CuK_α radiation (λ=1.54060 Å). The microstructural and elemental analyses were characterized using a Zeiss ULTRA 55 model scanning electron microscope (SEM) equipped with an energy dispersive spectroscopy (EDS) system. To determine the band gap energy was estimated from the optical absorption, which was measured by recording the transmission spectra using a UV-Visible spectrophotometer (Ocean Optics HR4000) coupled to an integrating sphere (in order to collect both specular and diffuse transmittance).

Photo electrochemical and electrochemical analyses

The PEC measurements were performed in a quartz cell to facilitate the light reaching the photo electrodes surface. The light exposed surface of the working electrode is 0.25 cm^2. The electrolyte used in all PEC measurements is 0.1 M Na_2SO_4. A potentiostat/galvanostat Autolab PGSTAT 302 N (Metrohm, Netherlands) with a Pt rod counter-electrode and an Ag/AgCl saturated in 3 M KCl reference electrode was used. The

chronoamperometry curves of the films were also obtained in dark and under illumination with an intensity of about 1 SUN (100 mW cm^{-2}) at the film surface.

Results and Discussion

Structural properties

The X-ray diffraction (XRD) patterns of Cu_2ZnSnS_4 quaternary alloy nanostructures as deposited, annealed in Ar and in sulfur atmosphere are shown in **Figure 1**. There are five peaks attributed to the diffractions of the (112), (101), (110), (105), and (312) planes, at 2θ=28.35°, 44.05°, 46.68°, 47.31°, 55.54° and 28.27°, 44.05°, 47.32°, 47.42°, 55.96°, respectively for Cu_2ZnSnS_4 annealed in sulfur and in Ar atmospheres. The Cu_2ZnSnS_4 (CZTS) nanostructures were found to consist of the tetragonal structure kesterite phase, with the (112), (105), (220) and (312) diffraction peaks corresponding to those of JSPDS card 26-0575.

XRD patterns shown in **Figure 1** with diffraction angle 2θ varied from 10 to 60 degrees. The observed peaks are attributed to both CZTS and ITO. However, the XRD pattern of the as deposited CZTS film shows the ITO characteristic peaks

only. After annealing in Ar atmosphere (without sulfur) the XRD pattern corresponds to the kesterite CZTS phase in addition to ITO peaks. Those annealed in sulfur atmosphere indicates a good crystallized kesterite phase and disappear of ITO peaks referring to successful growth of CZTS kesterite phase.

There is no peak for secondary phases in contrast to some reports states that copper sulfide, tin sulfide, and copper tin sulfide compounds exist as intermediates during sulfurization. Those secondary phase sulfides always form mixtures with CZTS at low sulfurization temperatures whereas they did not appear in the prepared CZTS films. This result is due to the selective process of precursor starting materials, sensitivity control of solution pHs and complexing agent concentration dependence. Careful equilibrium between temperature and annealing atmosphere thus in absence of sulfur we have increased the temperature of annealing to 450°C. In the same time, we have decreased annealing temperature in presence of sulfur to 400°C. Both annealing process were done for 45 min which is also in decrease with comparison to other stated work where the annealing temperature is set for 1 h or more.
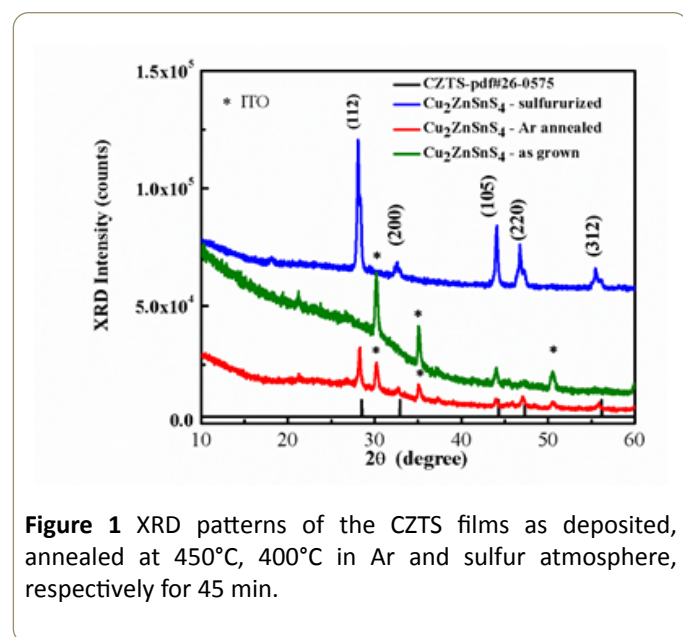
Figure 1 XRD patterns of the CZTS films as deposited, annealed at 450°C, 400°C in Ar and sulfur atmosphere, respectively for 45 min.

As the annealing process were done in different atmospheres as a function of time stability, lead to an optimized resultant CZTS kesterite phase. Crystallite size was calculated according to Scherer's formula:

$$D = k\lambda / \beta \cos\theta$$

where β is the Full Width at Half Maximum (FWHM), λ wavelength of X-rays with value is 1.5418 A, K is Scherer's constant depending on the crystallite shape and is close to 1 (K=0.9 was used) and θ is the Bragg angle at the center of the peak. **Table 2** displays the crystallite sizes for CZTS films annealed in Ar and in sulfur atmospheres, respectively.

Table 2 Crystallite size measurement of Cu_2ZnSnS_4 annealed in Ar atmosphere and sulfurized films.

Sample	Crystallite size (nm)
Cu_2ZnSnS_4 - Annealed in Ar	27.8
Cu_2ZnSnS_4 - sulfurized	17.3

It is worth to notice that the crystallite size of kesterite phase Cu_2ZnSnS_4 sulfurized ones has larger crystallite size than those annealed in Argon atmosphere. The annealing process in Argon atmosphere were held at 450°C which lead to complete kesterite phase formation with all kesterite indexed peaks in addition to those of ITO used substrate. In the mean while those grown in sulfur atmosphere shown sharp indexed peaks for kesterite phase only and no substrate ITO representative peaks.

Optical properties

Figure 2 shows the transmittance and absorbance spectra for the CZTS thin films as-grown and sulfurized, respectively. As can be seen the transmittance for the sulfurized sample is higher in all the studied wavelength range, meaning that the reflectance of the surface has decreased after the sulfurization process.
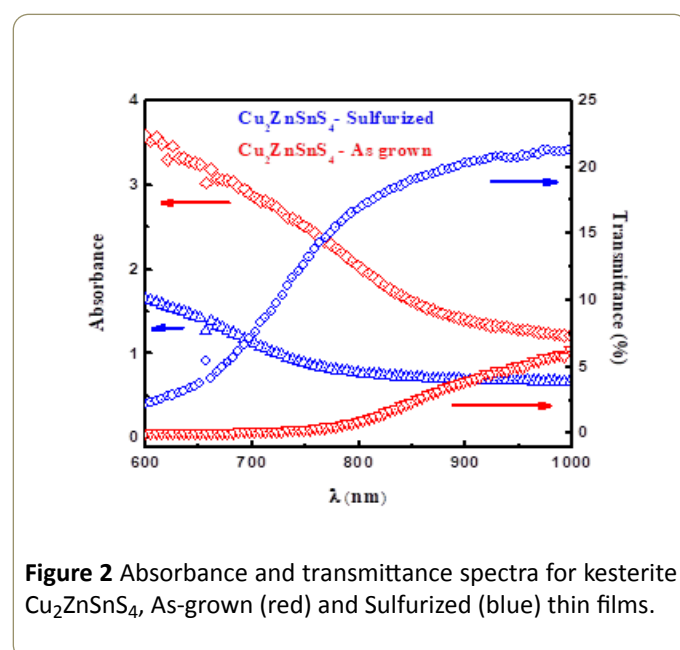

Figure 2 Absorbance and transmittance spectra for kesterite Cu_2ZnSnS_4, As-grown (red) and Sulfurized (blue) thin films.

For a direct-band-gap semiconductor, the optical band gap energy can be evaluated by the expression $(\alpha h)^2 = A(h - Eg)$, where Eg is the optical band gap energy, A is an energy independent constant, h is the Planck constant, υ is frequency, and n is an index that characterizes the optical absorption process and is theoretically equal to 1/2 for the direct allowed transitions.

All the CZTS thin film samples exhibited broad absorption in the visible region. The band gaps were obtained by plotting $(\alpha h \upsilon)^2$ versus the photon energy in eV. Extrapolation of the straight line to zero absorption coefficient ($\alpha = 0$) allows estimation of Eg.

Figure 3 shows the Tauc plot of Cu_2ZnSnS_4 kesterite thin films before annealing the (as grown) and sulfurized samples in

sulfur atmosphere. The band gaps of the as grown films were 1.83 eV and 1.52 eV for the sulfurized ones which is close to the reviewed CTZS band gap values.
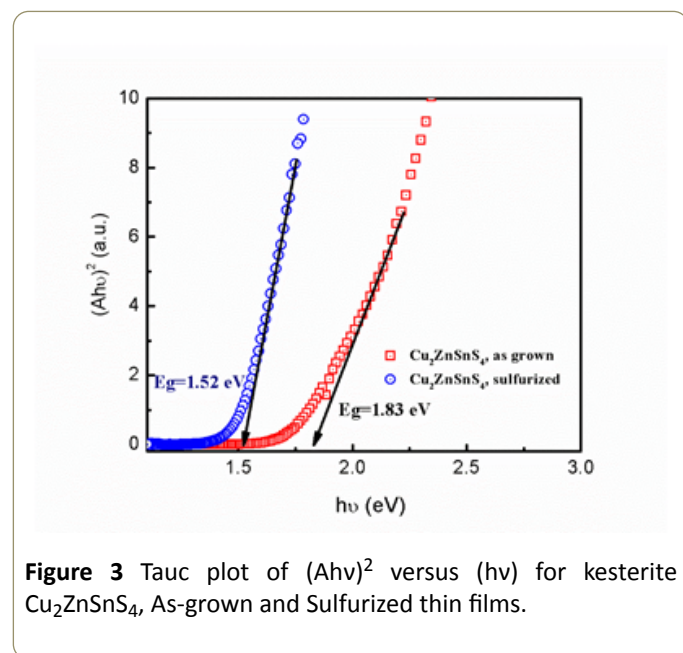
Figure 3 Tauc plot of $(Ah\nu)^2$ versus $(h\nu)$ for kesterite Cu_2ZnSnS_4, As-grown and Sulfurized thin films.

Scanning electron microscopy

Figure 4 shows Scanning Electron Microscopy (SEM) images of the sulfurized CZTS films at different magnifications. Scanning Electron Microscopy is one of the predominant techniques to survey the surface of the samples. The SEM analysis reveals that the grown films revealing good crystallinity in agreement with XRD data. Uniform, homogenous, well-covered and good adherence agglomeration of grains with the films. No secondary phases have been detected in contrast to annealing in sulfur atmosphere at low temperatures like, ZnS, SnS, CuSnS and CuS.
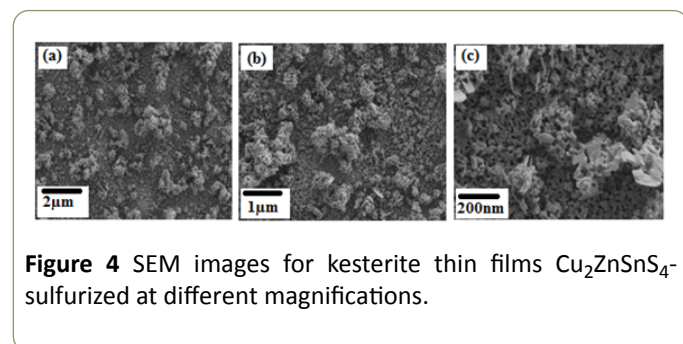
Figure 4 SEM images for kesterite thin films Cu_2ZnSnS_4-sulfurized at different magnifications.

The growth temperature determines growth of CZTS films presence of sulfur enhance the crystallinity of the films. The films deposited at 400°C in sulfur atmosphere show homogeneity with smooth islands or small grains owing to combination of CZTS formed in Ar atmosphere and sulfur. The smooth region is related to the stoichiometry of the pure kesterite CZTS formed phase with (Cu:Zn:Sn:S=2:1:1:4) ratio of constituent films which is highly required to develop efficient thin film solar cells. The SEM images of the sulfurized CZTS

films grown with optimum growth conditions show very uniform grain sizes.

EDS analysis

The composition of the as-deposited sample was evaluated by a quantitative EDS analysis. **Figure 5** shows a typical EDS spectrum revealing peaks of Cu, Zn, Sn and S, due to the deposited CZTS thin film. It is also obviously noticed that no presence of any additionally peaks arising from substrate ITO.

The fundamental properties of CZTS have proven to be suitable to serve as an active layer in solar cell devices. In the Cu-based chalcogenides the Cu content is of key importance, that it is strongly affects morphological, structural and electrical properties of the films. Therefore, as a first optimization for experimental conditions to synthesize CZTS, we studied structural and morphological properties of CZTS thin films as well as corresponding solar cell parameters by varying the content of Cu. Controlling the amount of copper lead to varying all other constituent elements, which in turn lead to varying all other elemental ratios: i.e., Zn/Sn, (Cu/(Zn+In) and (S/metal) ratios.

Figure 5 shows a typical EDS spectrum of sulfurized films. Peaks corresponding to the four components Cu, Zn, Sn, and S of CZTS films are evident in ECS spectrum.
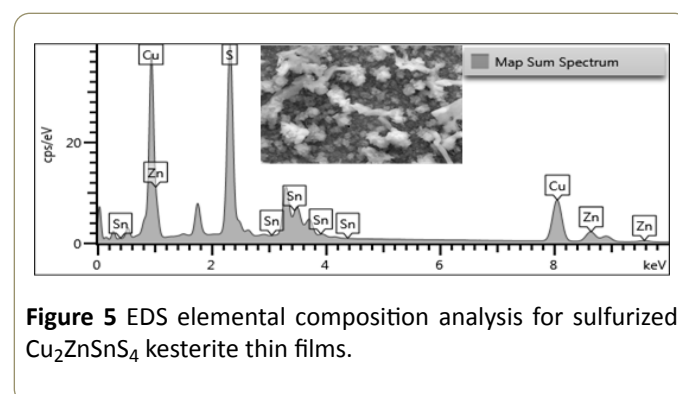
Figure 5 EDS elemental composition analysis for sulfurized Cu_2ZnSnS_4 kesterite thin films.

The composition of the studied samples is presented in the **Table 3** and their relative positions are indicated in the phase diagram **(Figure 5)**. The calculated ratios [Cu]/([Zn]+[Sn])=0.5 and [Zn]/[Sn]=1.4, where the [s]/([metal]) ratio is equal to 1.65; which is clearly the most effected one due to the high ratio of sulfur more than 50%. The apparent composition of the elements is 12.59 at%, 14.79 at%, 10.27 at% and 62.32 at % for Cu, Zn, Sn, and S elements, respectively. In general, it has been observed that sulfurized films are moderately poor in Cu and rich in S. The calculated [Cu]/([Zn]+[Sn])=0.5 and [Zn]/[Sn]=1.4, where the [s]/([metal]) ratio is equal to 1.65; which is clearly the most effected one due to the high ratio of sulfur more than 50%.

Table 3 Compositional analysis of sulfurized Cu_2ZnSnS_4 kesterite thin films.

| Elements composition atomic (%)	Elemental composition ratio

	Cu (%)	Zn (%)	Sn (%)	S (%)	Cu/Zn +Sn	Zn/S n	S/ metal
$Cu_2Zn SnS_4$	12.5 9	14.7 9	10.2 7	62.3 5	0.5	1.4	1.65

Photo electrochemical measurements of CZTS

Photo electrochemistry has been employed to explore the semiconducting properties of sulfurized Cu_2ZnSnS_4. When semiconductor electrodes are exposed to periodic illumination, the current driven is affected by the creation of electron-hole pairs, which alters the concentration of minority carriers and thereby promotes processes governed by these carriers. During photoexitation both photopotential and photocurrent can be observed, even at open circuit potential. The photo excited electrons and holes are separated in the space charge layer, and are driven by the electric field in opposite directions. This migration induces an inverse potential in the electrode (photopotential), reducing the potential difference across the space charge layer and retarding the migration of the carriers. In the case of p-type semiconductors, the Fermi level of the semiconductor decreases (the electrode potential increases) when the band edge level bends downward in the space charge layer. Moreover a negative photocurrent is registered when photogenerated electrons move across the space charge region towards the electrode/electrolyte interface and increase the cathodic current [11].

Figure 6 shows the photocurrent registered at open circuit potential and the photopotential developed across the sulfurized CZTS at 400°C. The cathodic nature of the photocurrent and the positive value of the photopotential confirm the p-type character of the sulfurized CZTS film.
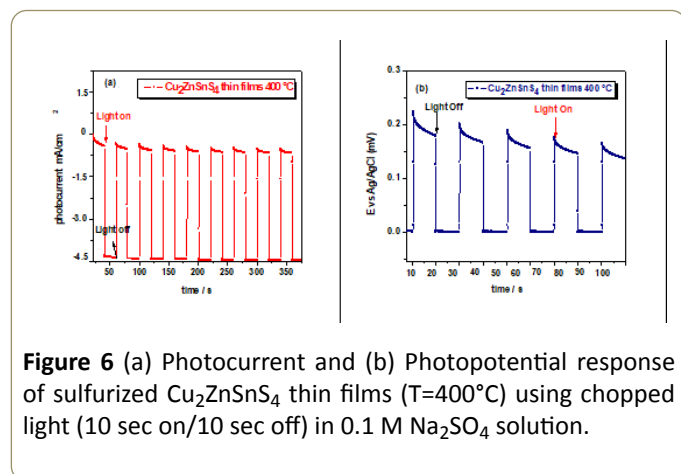
Figure 6 (a) Photocurrent and (b) Photopotential response of sulfurized Cu_2ZnSnS_4 thin films (T=400°C) using chopped light (10 sec on/10 sec off) in 0.1 M Na_2SO_4 solution.

Conclusion

Cu_2ZnSnS_4 thin films with kesterite structure were successfully synthesized using single step electrodeposition process. Annealing process in Argon and sulfur atmosphere were studied as function of time, as the time was fixed where in Argon atmosphere the temperature was held higher than those in sulfur atmosphere.

Characterization techniques have revealed the formation of pure kesterite phase for the prepared Cu_2ZnSnS_4 films in both argon and sulfur atmosphere. XRD structure study showed indexed peaks for Cu_2ZnSnS_4 thin films with kesterite structure with average crystal size about 17 nm.

The morphological study for the sulfurized samples indicates that both films are polycrystalline with a uniform homogenous surface morphology suitable for solar cell applications. The elemental EDS analysis promotes that the prepared sulfurized films with Cu poor, Zn and S rich Cu_2ZnSnS_4 sulfurized kesterite films. For the photoelectrochemical performance of the Cu_2ZnSnS_4 the photocurrent registered at open circuit potential and the photopotential developed across the sulfurized CZTS at 400°C improve the cathodic nature of the photocurrent and the positive value of the photopotential confirms the p-type character of the film.

Acknowledgements

References

1. Repins I, Beall C, Vora V, DeHart C, Kuciauskas D, et al. (2012) Co-evaporated $Cu_2ZnSnSe_4$ films and devices. Sol Energy Mater Sol Cells 101: 154-159.

2. Dudchak IV, Piskach LV (2003) Phase equilibria in the Cu_2SnSe_3–$SnSe_2$–ZnSe system. J Alloys Compd 351: 145-150.

3. Chen S, Gong XG, Walsh A, Wei SH (2009) Electronic structure and stability of quaternary chalcogenide semiconductors derived from cation cross-substitution of II-VI and I-III-VI compounds. Phys Rev B 79: 165211.

4. Persson C (2010) Electronic and optical properties of Cu_2ZnSnS_4 and $Cu_2ZnSnSe_4$. J Appl Phys 107: 053710.

5. Shin B, Gunawan O, Zhu Y, Bojarczuk NA, Chey SJ, et al. (2013) Thin film solar cell with 8.4% power conversion efficiency using an earth-abundant Cu_2ZnSnS_4 absorber. Prog Photovoltaics 21: 72-76.

6. Siebentritt S (2013) Why are kesterite solar cells not 20% efficient? Thin Solid Films 535: 1-4.

7. Watjen JT, Engman J, Edoff M, Bjorkman CP (2012) Direct evidence of current blocking by ZnSe in $Cu_2ZnSnSe_4$ solar cells. Appl Phys Lett 100: 173510.

8. Scragg JJ, Wätjen JT, Edoff M, Ericson T, Kubart T, et al. (2012) A Detrimental Reaction at the Molybdenum Back Contact in Cu_2ZnSn (S, Se)$_4$ Thin-Film Solar Cells. J Am Chem Soc 134: 19330-19333.

9. Ahn S, Jung S, Gwak J, Cho A, Shin K, et al. (2010) Determination of band gap energy (Eg) of $Cu_2ZnSnSe_4$ thin films: On the discrepancies of reported band gap values. Appl Phys Lett 97: 021905.

10. Redinger A, Hoenes K, Fontane X, Roca VI, Saucedo E, et al. (2011) Detection of a ZnSe secondary phase in coevaporated $Cu_2 ZnSnSe_4$ thin films. Appl Phys Lett 98: 101907.

11. Scragg JJ, Berg DM, Dale PJ (2010) A 3.2% efficient Kesterite device from electrodeposited stacked elemental layers. J Electroanal Chem 646: 52-59.

12. Lee SG, Kim J, Woo HS, Jo Y, Inamdar AI, et al. (2014) Structural, morphological, compositional, and optical properties of single step electrodeposited Cu_2ZnSnS_4 (CZTS) thin films for solar cell application. Curr Appl Phys 14: 254-258.

13. Gunaicha PP, Gangam S, Roehl JL, Khare SV (2014) Structural, energetic and elastic properties of Cu_2ZnSn (SxSe1-x) 4 (x=1, 0.75, 0.5, 0.25, 0) alloys from first-principles computations. Sol Energy 102: 276-281.

14. Seol JS, Lee SY, Lee JC, Nam HD, Kim KH (2003) Sol Energy Mater Sol Cells 75: 155.

15. Katagiri H, Jimbo K, Maw WS, Oishi K, Yamazaki M, et al. (2009) Thin Solid Films 517: 2455-2460.

16. Fernandes PA, Salome PMP, Cunha AFDA (2011) Cu_2ZnSnS_4 solar cells prepared with sulphurized dc-sputtered stacked metallic precursors. Thin Solid Films 519: 7382-7385.

17. Vora N, Blackburn J, Repins I, Beall C, To B, et al. (2012) Phase identification and control of thin films deposited by co-evaporation of elemental Cu, Zn, Sn, and Se. J Vac Sci Technol 30: 051201.

18. Shin B, Gunawan O, Zhu Y, Bojarczuk NA, Chey SJ, et al. (2013) Thin film solar cell with 8.4% power conversion efficiency using an earth-abundant Cu_2ZnSnS_4 absorber. Prog Photovoltaics Res Appl 21: 72.

19. Repins I, Beall C, Vora N, Dehart C, Kuciauskas D, et al. (2012) Sol Energy Mater Sol Cells 101: 154.

20. Knutson TR, Hanson PJ, Aydil ES, Penn RL (2014) Synthesis of Cu_2ZnSnS_4 thin films directly on to conductive substrates via selective thermolysis using microwave energy. Chem Commun 50: 5902.

21. Scragg JJ, Berg DM, Dale PJ (2010) A 3.2% efficient Kesterite device from electrodeposited stacked elemental layers. J Electroanal Chem 646: 1-2.

22. Schurr R, Hölzing A, Jost S, Schock HW (2009) The crystallisation of Cu_2ZnSnS_4 thin film solar cell absorbers from co-electroplated Cu-Zn-Sn precursors. Thin Solid Films 517: 2465-2468.

23. Todorov TK, Reuter KB, Mitzi DB (2010) High-efficiency solar cell with Earth-abundant liquid-processed absorber. Adv Mater 22: E156-159.

24. Fahrettin Y (2011) Nanostructure Cu_2ZnSnS_4 Thin Film Prepared By Sol-gel For Optoelectronic Applications. Solar Energy 85: 2518–2523.